In-situ synthesis of poly(dimethylsiloxane)–gold nanoparticles composite films and its application in microfluidic systems†

Qing Zhang, Jing-Juan Xu,* Yan Liu and Hong-Yuan Chen*

Received 19th June 2007, Accepted 25th October 2007
First published as an Advance Article on the web 14th November 2007
DOI: 10.1039/b716295m

We presented a simple approach for *in-situ* synthesis of poly(dimethylsiloxane) (PDMS)–gold nanoparticles composite film based on the special characteristics of PDMS itself. It is an environmentally safe synthesis method without the requirement of additional reducing/stabilizing agents. The region where the resulting gold nanoparticles distribute (in the matrix or on the surface of the polymer) and the size of the nanoparticles, as well as the colour of the free-standing films, can be simply controlled by adjusting the ratio of curing agent and the PDMS monomer. The chemical and optical properties of these composite films were studied. Using such a method, gold nanoparticle micropatterns on PDMS surfaces can be performed. And based on the gold nanoparticles micropattern, further modification with antibodies, antigens, enzymes and other biomolecules can be achieved. To verify this ability, an immobilized glucose oxidase (GOx) reactor in microchannels was built and its performance was studied. The experiments have shown that the resulting composite film may have a lot of potential merits in protein immobilization, immunoassays and other biochemical analysis on PDMS microchips.

Introduction

Poly(dimethylsiloxane) (PDMS) is one of the most widely used polymer materials for fabricating microfluidic chips due to its transparency, outstanding elasticity, good thermal and oxidative stability, ease to be fabricated and sealed with various materials.[1] In spite of these advantages, PDMS is not a "faultless" material in its applications of microfluidic chips.[2,3] For example, the surface of PDMS is inert, which results in the difficulty in introducing biomolecules, such as enzymes, antibodies, nucleic acids, and proteins, into PDMS microfluidic chips. It greatly limits the use of PDMS in on-chip bioassays based on immobilized biomolecules. To resolve this problem and expand the applications of PDMS microfluidic chips, chemical modification layers,[4,5] sol-gel[6] and nano- or microparticles[7] have been introduced to PDMS microchannels.

Recently, nanocomposites consisting of metal nanoparticle doped polymer matrices, especially free-standing nanoparticles–polymer films,[8–13] have attracted enormous interest in both the science and technology fields, due to their potential applications in optical devices[14], microelectromechanical devices[15] and biosensors.[16,17] Metal nanoparticles–PDMS composite films can be used to fabricate optical film,[18] color transition devices[19] and surface-enhanced Raman scattering (SERS) substrate.[20] PDMS microchips modified with nanoparticles can obtain enhanced electrophoretic performance[21] and be used to bind biomolecules for on-chip immunoassay.[22] In these reports, there are two approaches to fabricate metal nanoparticles–PDMS composite films. One approach is to firstly mix solutions of nanoparticles with PDMS precursors, and then remove the solvents and cure the mixture to obtain composite films with nanoparticles uniformly dispersed in PDMS matrix. The other one is to immobilize nanoparticles on pre-treated PDMS surface. This method is often used to introduce nanoparticles to microchips. In both cases, nanoparticles should be synthesized preliminarily. Recently, Wang and co-workers[23] have reported a surface synthesis method for fabricating gold nanoparticles–PDMS films. A reducing and stabilizing agent, chitosan, was first coated on PDMS surface, and then the coated PDMS was immersed in $HAuCl_4$ solution to form gold nanoparticles on its surface.

Here, a simple approach is presented for *in-situ* preparation of gold nanoparticles–PDMS free-standing films, without the need of additional reducing agent. The residual curing agent in PDMS matrix itself is used to reduce $HAuCl_4$. The resulting composite film has some interesting characteristics and may be used in optical devices, immunoassays and other bioassays on PDMS-based microchips. For example, the gold nanoparticles patterned PDMS, followed by surface derivatization can be easily used to fabricate microfluidic immobilized enzyme reactors. Moreover, Ag–PDMS composite film could be also synthesized using such method.

Key Laboratory of Analytical Chemistry for Life Sciences, School of Chemistry and Chemical Engineering, Nanjing University, Nanjing, China 210093. E-mail: xujj@nju.edu.cn; hychen@nju.edu.cn; Fax: +86-25-83594862; Tel: +86-25-83594862

† Electronic supplementary information (ESI) available: Scheme of PDMS crosslinking reaction, ATR-FT-IR spectra of the PDMS film with different η, TEM image of the cross section of the Au nanoparticles–PDMS films and data of Ag nanoparticles–PDMS free-standing film. See DOI: 10.1039/b716295m

Experimental

Materials and reagents

The Sylgard 184 (including PDMS monomer and curing agent) was purchased from Dow Corning (Midland, MI, USA). $HAuCl_4 \cdot 4H_2O$ was from Shanghai Chemical Reagent Company (Shanghai, China). Glucose oxidase (Gox) and

Dithiobis-*N*-succinimidyl-propionate (DTSP) was purchased from Sigma (St. Louis, MO, USA). Glucose was from Shanghai Bio Life Science & Technology (Shanghai, China). All other chemicals were of analytical grade and used without further purification. All solutions were prepared with doubly distilled water and passed through a 0.22 μm cellulose acetate filter.

Synthesis of the gold nanoparticles–PDMS composite film

To synthesize nanoparticles–polymer composite films, PDMS monomer and the curing agent (Sylgard 184, Dow Corning, USA) were firstly mixed in a certain proportion mentioned in the text and cured at 80 °C for 90 min. The resulting native PDMS thin films were immersed in 0.5% (m/v) $HAuCl_4$ aqueous solution (or drop the $HAuCl_4$ solution on the PDMS films) and incubated at room temperature for a certain time.

Region-selective synthesis of gold nanoparticles on the surface of PDMS chips

Using microchannels. The masters of PDMS microchannels were fabricated using an office laser printer according to our previous work.[24] To fabricate gold nanoparticle patterns, PDMS chips with different patterns were sealed with another PDMS substrate to form enclosed microchannels, with a hole being punched at one end of the patterns acting as a solution reservoir. Then, 0.5% (m/v) $HAuCl_4$ solution was introduced into the microchannels by vacuum and incubated for 48 h.

Using oxygen plasma. The desired region on the substrate of PDMS chips was firstly covered with a mask (can be made of PDMS or other materials) and then treated in a plasma cleaner (PDC-32G, Harrick, USA) for 60 s. After taking off the mask, the PDMS substrate was immersed in 0.5% (m/v) $HAuCl_4$ aqueous solution and incubated at room temperature for a certain time.

Binding of antibody–antigen and immobilization of enzyme. For antibody–antigen binding, mouse IgG and FITC-tagged anti-mouse IgG (Jackson ImmunoResearch Laboratories, Inc.) were dissolved in 20 mM phosphate buffer solution (pH 7.0). A 0.1 mg ml^{-1} solution of mouse IgG was added to the surface of gold nanoparticles patterned PDMS and incubated overnight at 4 °C, followed by rinsing with doubly distilled water and drying with pure nitrogen gas. Then, a 25 ug ml^{-1} solution of anti-mouse IgG was added to the surface for 2 h at room temperature, again followed by rinsing with doubly distilled water and drying with pure nitrogen gas. Finally, the film was analyzed using a DMIRE2 inverse fluorescence microscope (Leica, Germany).

For enzyme immobilization, DTSP was used as an anchor.[25] A 4.0 mM solution of DTSP in dimethyl sulfoxide (DMSO) was added to the surface of the gold nanoparticles patterned PDMS microchannel and incubated for 1 h at room temperature. The PDMS plate was thoroughly washed with acetone and 20 mM phosphate buffer, respectively. Then it was dried under nitrogen gas. Afterwards, a 4.0 mg ml^{-1} solution of GOx in 20 mM phosphate buffer was added to the surface of the PDMS plate and incubated for 24 h at 4 °C. Again, it was washed with acetone and 20 mM phosphate buffer, and followed by drying under nitrogen gas. Finally, it was sealed with another clear PDMS substrate to form an enclosed chip and stored in phosphate buffer at 4 °C before use. The layout of the microchip is shown in Fig. 1. The width and the length of the sample channel are 150 μm and 16 mm, and the separation channel are 200 μm and 35 mm, respectively. The length of immobilized enzyme region was 25 mm. The height of the channels was identical for *ca.* 10 μm.

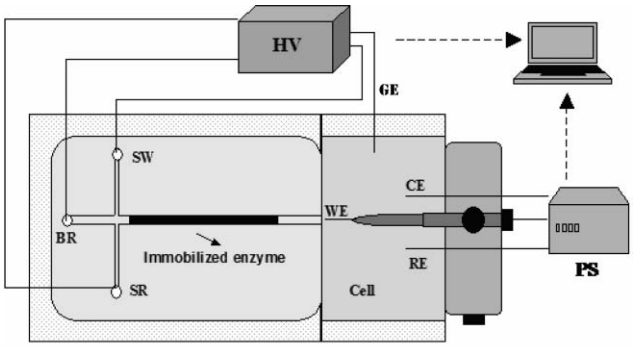

Fig. 1 Schematic diagram of high voltage, (PC) personal computer, (WE) working electrode, (CE) counter electrode, (RE) reference electrode, (GE) ground electrode, (BR) buffer reservoir, (SR) sample reservoir, (SW) sample waste, and (Cell) detection cell.

Microchip electrophoresis. The PDMS microchip was placed on a home-made Plexiglas holder integrated with a precise 3-D adjustor for precisely positioning the working electrode. A home-made power supply with voltage ranging from 0 to 5000 V was used to provide high voltage. Amperometric detection was performed with an Electrochemical Workstation 660A (CH Instruments, Austin, TX, USA). The detector cell was integrated in the Plexiglas holder. A carbon fiber cylindrical electrode with a diameter of 8 μm was used as a working electrode, combining an Ag/AgCl reference electrode and a Pt wire auxiliary electrode to construct a three-electrode system as our previous report.[26] The schematic diagram of the whole device is shown in Fig. 1.

Results and discussion

Synthesis of the gold nanoparticles–PDMS composite film

As well-known, PDMS is one of the most popular materials for fabrication of micropattern and microfluidic channels. Also, PDMS is one of the most permeable rubbery polymers, which is used in membrane-based separation applications of vapor[27,28] or small molecules.[29] The crosslinking of PDMS is based on the reaction between silicon hydride (Si–H) groups in the curing agent and vinyl groups ($Si–CH=CH_2$) in the monomer[30] (see Scheme 1S in ESI†). In the cured PDMS, there remains some Si–H group and its concentration was controlled by the mass ratio of the curing agent and the monomer (η). The greater η results in a higher concentration of the residual Si–H group (see Fig. 1S in ESI†).

When a native PDMS film was immersed in $HAuCl_4$ solution, the film became red gradually, indicating gold

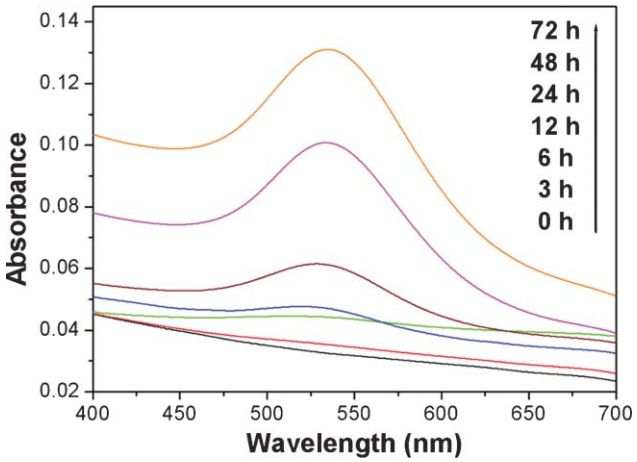

Fig. 2 UV-Vis spectra of PDMS film incubated in 0.5% (m/v) $HAuCl_4$ solution with different incubation times, performed on a SHIMADZU UV-3100 UV-Vis-NIR recording spectrophotometer. η was 0.1.

nanoparticles were formed. UV-Visible absorption spectroscopy was used to monitor the plasmon absorption of gold nanoparticles produced. The dependence of the UV-Vis spectra of the PDMS film incubated in the $HAuCl_4$ solution on different incubation times is shown in Fig. 2. The absorption band centred at 530–534 nm results from the surface plasmon band of gold nanoparticles.[23] The absorption intensity increased with incubation time, indicating the formation and increasing population of gold nanoparticles.

In the formation process of gold nanoparticles, no introduction of other reagents but PDMS matrix and $HAuCl_4$ was used. The residual Si–H group in PDMS film was considered to act as the direct reduction reagent to reduce $HAuCl_4$. This presumption has been proven by the attenuated total reflection (ATR) of FT–IR spectra (Fig. 3). In the ATR-FT-IR spectra, the absorption peak of the Si–H group

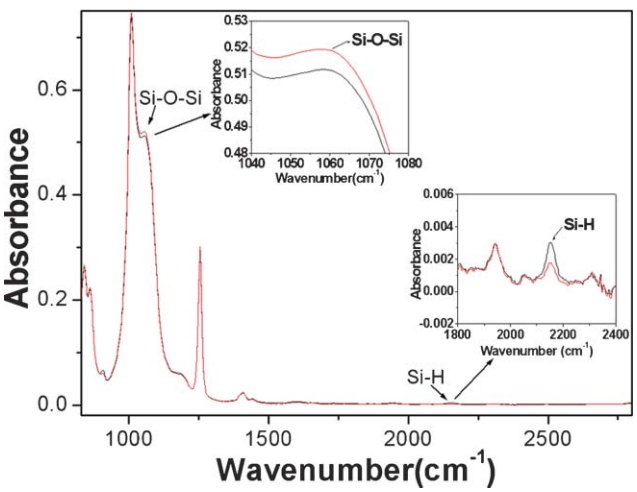

Fig. 3 ATR–FT–IR spectra for a native PDMS film (black line) and after the PDMS film incubated in 0.5% (m/v) $HAuCl_4$ aqueous solution for 48 h (red line), performed on a BRUKER IFS 66/S time resolved FT-IR spectroscope.

of PDMS was observed at 2154 cm^{-1}. As the nanoparticles formed in the PDMS film, the intensity of this absorption peak of Si–H group decreased, which revealed that some of the Si–H groups had been consumed. On the other hand, the intensity of the absorption peak of the Si–O–Si group was found to increase at 1060 cm^{-1}.

Thus the possible reaction between Si–H groups and $HAuCl_4$ can be described as:

$$3\,\mathrm{Si}-\mathrm{H}+3/2\mathrm{H_2O}+2\mathrm{AuCl_4^-}\rightarrow 3/2-\mathrm{Si}-\mathrm{O}-\mathrm{Si}-2\mathrm{Au}+8\mathrm{Cl^-}+6\mathrm{H^+}$$

Transmission electron microscopy (TEM) images (see Fig. 2S in ESI†) provided essential evidence about the formation process. Gold nanoparticles existed in a thin surface layer with the thickness of *ca.* two microns (η was 0.06 and the incubation time was 48 h). It indicated that the network structure of PDMS allows $AuCl_4^-$ to diffuse into its matrix. Therefore, the process can be described as follows: when the PDMS film contacted with the $HAuCl_4$ solution, the anions of $AuCl_4^-$ slowly diffused into the inside and reacted with the residual Si–H groups, resulting in the formation of gold nanoparticles. On the other hand, the PDMS polymer matrix could protect gold nanoparticles from aggregation. Therefore, the synthesis may be considered as a combined effect of curing agent and matrix of PDMS. Using this approach, we also prepared Ag–PDMS nanocomposite free-standing film by immersing the PDMS film in 15 mM $AgNO_3$ solution (see Fig. 3S in ESI†).

Controlling morphology of the composite films

The morphology of the composite films can be simply controlled by adjusting η, which is the most important factor for the synthesis of gold nanoparticles. It decides the region where the nanoparticles exist, and the appearance of the composite films. As it can be seen in Fig. 4a, when η was low (0.06 and 0.1), the composite films were transparent with different colors and most of the nanoparticles were individually dispersed in the polymer matrix. When a higher η (*e.g.* 0.15 or 0.18) was used, the resulting film was semi-transparent and most nanoparticles were on the surface. Apparently, at higher η values, a mass of residual Si–H groups existed on the PDMS surface. $AuCl_4^-$ anions can quickly react with the Si–H group on the surface and results in a great collection of Au nanoparticles. When the nanoparticles on the surface were peeled off by mechanical attrition, a colorless PDMS film was obtained (Fig. 4a, inset). It indicated that the produced nanoparticles on the surface block subsequent $AuCl_4^-$ anions entering the inner matrix of PDMS. This has also been proven by scanning electron microscopy (SEM) images (Fig. 5). The differences can also be observed in the UV-Vis spectra. As it can be seen in Fig. 4b, the maximum absorption peak shifts from 522 nm to 534 nm, with the increase of η from 0.06 to 0.1. When η keeps increasing, the shape of the nanoparticles becomes irregular as a result of the aggregation on the surface. Correspondingly, broad absorption peaks were observed in UV-Vis spectra (Fig. 4b).

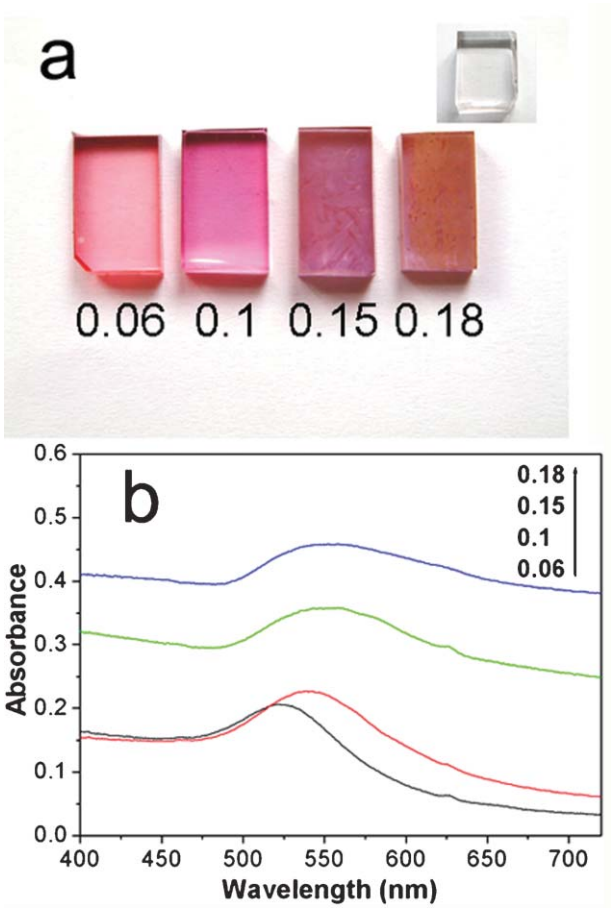

Fig. 4 (a) Photographic images of the PDMS–gold nanoparticles free-standing films with different η, the incubation time is 48 h. The image at the top right corner is the film (η = 0.18) peeled off the nanoparticles on its surface by mechanical attrition. (b) UV-Vis spectra of the PDMS–gold nanoparticles free-standing films with different η.

The ratio of the curing agent and the monomer also has a great effect on the shape and size of the gold nanoparticles. When η was 0.06, the mean diameter of the gold nanoparticles

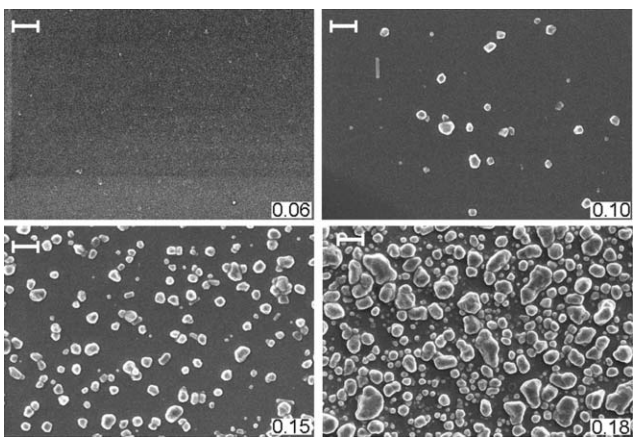

Fig. 5 SEM images of the PDMS–gold nanoparticles free-standing films with different η, performed on a JEOL JSM-6700F field emission scanning electron microscope at an accelerating voltage of 5 kV. Scale bar =1 μm.

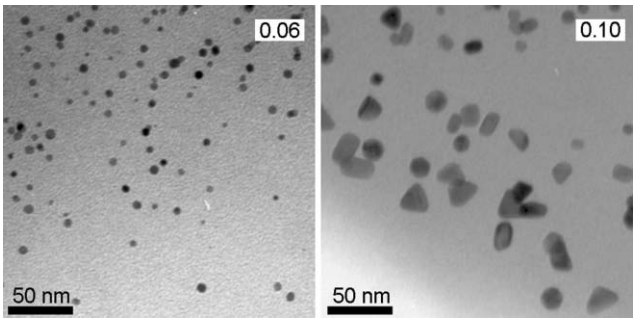

Fig. 6 TEM images of the PDMS–gold nanoparticles with different η, obtained using a JEOL JEM-1230 transmission electron microscope. A gold nanoparticles doped PDMS slice with a thickness of 50 nm prepared by length cutting with an ultramicrotome was used for this electron-micrograph.

was 7 nm and the shape of most nanoparticles seemed to be round. When η was 0.1, the mean diameter increased to 13 nm and the shape was changed to polygonal, including triangles, rectangles, pentagons and hexagons (Fig. 6).

Color transition of the composite film

Polymers containing noble-metal nanoparticles have gained extensive scientific interest in some optical fields, since they exhibit some special optical properties, such as dichroism[14] and switching of optical properties.[19,31] In this work, the proposed nanocomposite films also have an interesting color transition phenomena (Fig. 7). When the PDMS film (η = 0.06) was incubated in $HAuCl_4$ solution for 48 h at room temperature, the color of the composite film was pale red. If the incubation time is as long as a week, the color would become violet red. It is due to the fact that the number of nanoparticles in the PDMS matrix would increase with the incubation time, and the adjacent nanoparticles would aggregate if the incubation time is too long. Remarkably, when the violet red film was immersed in diisopropylamine the color of the swollen film returned to pale red. When the

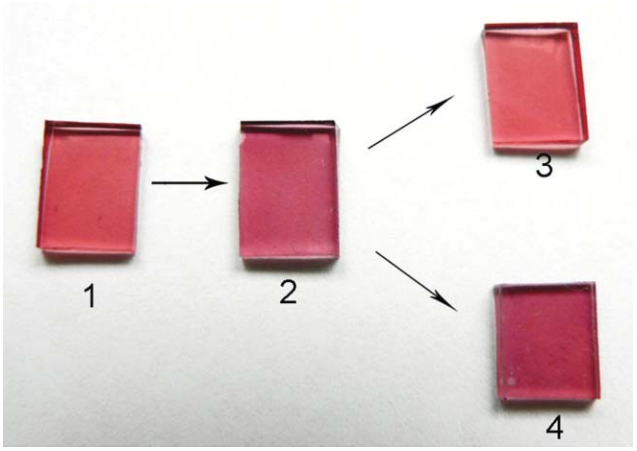

Fig. 7 Photographic images of PDMS films after incubated in 0.5% (m/v) $HAuCl_4$ aqueous solution for 2 days (1) and 7 days (2), the 7 day incubation film was immersed in diisopropylamine for 30 min and then dried under hot airflow (3) or at room temperature circumstance (4).

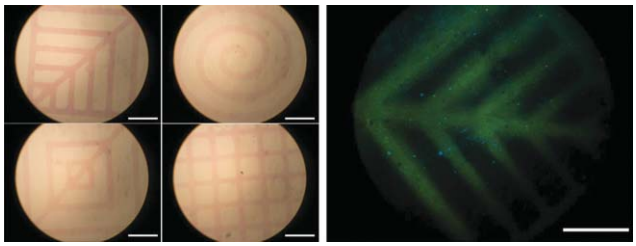

Fig. 8 (a) Photographic images of the gold nanoparticle patterns on PDMS chips. (b) Fluorescence image of FITC-tagged anti-mouse IgG in IgG–gold nanoparticles pattern. Scale bar = 1 mm.

swollen red film was dried naturally at room temperature conditions, the color turned to violet red again. However, when it was dried under hot airflow, the color was still pale red. This change is based on the solvent swelling and the solvent-dependent drying kinetics. Diisopropylamine is a very strong solvent to swell PDMS, and the nanoparticles would re-disperse in the swollen PDMS to show pale red color. When the solvent evaporated rapidly, the nanoparticles have no enough time to aggregate again and the color was then preserved.

Patterning gold nanoparticles on PDMS chips

Based on this *in-situ* synthesis method, there are two approaches to patterning gold nanoparticles on PDMS chips (Fig. 8(a)). One approach is to employ microchannel networks. $HAuCl_4$ solution was introduced into a microchannel and allowed to react only with the contactile region on the PDMS chips to form gold nanoparticle patterns. Another approach is to employ oxygen plasma. Oxygen plasma would cause the PDMS surface to form a SiOx silica-like layer that would extremely reduce the permeability of PDMS.[32] On the other hand, the residual Si–H group on the surface would beconsumed by the oxidation with oxygen plasma. Therefore, the PDMS surface becomes non-reactive to $HAuCl_4$ after it was treated with oxygen plasma. Masks (made of PDMS or other materials that can be tightly sealed with PDMS) were used to protect the desired region on PDMS surface during the treatment of oxygen plasma before it reacted with $HAuCl_4$. This would result in the fabrication of gold nanoparticle patterns.

Protein immobilization and microfluidic immobilized enzyme reactor

It is well known that a gold nanoparticle is a good substrate to be functionalized with antigen, enzymes and other biomolecules.[33–38] Therefore, the gold nanoparticle patterns on PDMS may have the application potential in immunoassays, biosensors and immobilized enzyme reactors on the PDMS microchips. To testify the capability, the antibody–antigen binding was performed on these films. Mouse IgG was firstly attached to gold nanoparticles patterned on the PDMS film. Then anti-IgG conjugated with FITC was exposed to the film, binding specifically to the attached IgG. This binding was visualized with a fluorescent microscope, shown in Fig. 8(b).

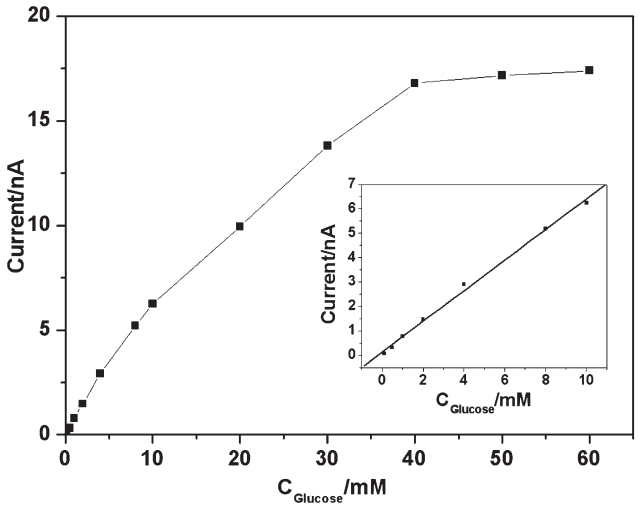

Fig. 9 Calibration curve of the response of the enzyme microreactor in PDMS microchip to glucose concentration. Inset shows the linear part of the calibration curve. Conditions: separation voltage: 650 V; sample injection: at 200 V for 3 s; the detection potential: 1.0 V

Based on surface derivatization of gold nanoparticles, we also built an immobilized GOx reactor on part of the separation channel. Taking glucose as a substrate, electroosmotic flow as a driving force and amperometry as a detection method, the performance of the reactor was studied. The running buffers used in the experiments were phosphate buffer (20 mM, pH 7.0). Before detection, the enclosed PDMS chip was filled with the running buffer by vacuum and flushed under an electric field until the separation and injection currents leveled off. Glucose solutions were added in the sample reservoir and electrokinetically injected into the microchannels. They were enzymatically oxidized with dissolved oxygen in the buffer solution and formed hydrogen peroxide, which can be detected at the working electrode. Fig. 9 shows the peak current of hydrogen peroxide as a function of the concentration of glucose. The current response increased linearly with the concentration of glucose lower than 10 mM (r = 0.998).

Conclusions

In this work, we have reported a self-sustaining synthesis of gold nanoparticles in PDMS for the first time. And a stable, robust and morphology controllable free-standing film of the Au–PDMS composite can be obtained using such an *in-situ* approach. Based on this method, gold nanoparticles can be easily introduced to PDMS microfluidic chips to immobilize biomolecules for the application of enzyme reactors, immunoassays and other biochemical analysis on microchips, although the distribution of gold nanoparticles on the PDMS surface are random at higher η. And the gold nanoparticle micropatterns can be used to address arrays of immobilized enzyme reactors in microfluidic chips.

PDMS is a familiar material to us but also with some unfamiliar features waiting for exploration. Digging at its unfamiliar features may find new ways to use it. We believe our work may give some new ideas about how to use PDMS in microfluidic chips.

Acknowledgements

This work was supported by the National Natural Science Foundation of China (No. 90206037, 20635002, 20475025, 20435010, 20575029), the National Natural Science Funds for Creative Research Groups (20521503), the 973 Program (2006CB933201, 2007CB936404) of China and the key project of the Science and Technology Research of MOE (106080).

References

1 J. C. McDonald and G. M. Whitesides, *Acc. Chem. Res.*, 2002, **35**, 491.
2 S. K. Sia and G. M. Whitesides, *Electrophoresis*, 2003, **24**, 3563.
3 H. Makamba, J. H. Kim, K. Lim and N. Park, et al., *Electrophoresis*, 2003, **24**, 3607.
4 D. A. Markov, K. Swinney and D. J. Bornhop, *J. Am. Chem. Soc.*, 2004, **126**, 16659.
5 H. L. Wu, J. J. Zhai, Y. P. Tian and H. J. Lu, et al., *Lab Chip*, 2004, **4**, 588.
6 J. Heo and R. M. Crooks, *Anal. Chem.*, 2005, **77**, 6843.
7 Q. Zhang, J. J. Xu and H. Y. Chen, *Electrophoresis*, 2006, 4943.
8 S. Porel, S. Singh, S. S. Harsha, D. N. Rao and T. P. Radhakrishnan, *Chem. Mater.*, 2005, **17**, 9.
9 S. Porel, S. Singh and T. P. Radhakrishnan, *Chem. Commun.*, 2005, **18**, 2387.
10 N. Watanabe, J. Morais, S. B. B. Accione, A. Morrone, J. E. Schmidt and M. C. M. Alves, *J. Phys. Chem. B*, 2004, **108**, 4013.
11 S. T. Selvan, J. P. Spatz, H. A. Klok and M. Moller, *Adv. Mater.*, 1998, **10**, 132.
12 I. Hussain, M. Brust, A. J. Papworth and A. I. Cooper, *Langmuir*, 2003, **19**, 4831.
13 K. Mallick, M. J. Witcomb and M. S. Scurrell, *Eur. Polym. J.*, 2006, **42**, 670.
14 Y. Dirix, C. Bastiaansen, W. Caseri and P. Smith, *Adv. Mater.*, 1999, **11**, 223.
15 H. Chen, X. Liu, H. Muthuraman, J. Zou, J. Wang, Q. Dai and Q. Huo, *Adv. Mater.*, 2006, **18**, 2876.
16 M. T. Sulak, O. Gokdogan, A. Gulce and H. Gulce, *Biosens. Bioelectron.*, 2006, **21**, 1719.
17 Y. Z. Xian, Y. Hu, F. Liu, Y. Xian, H. T. Wang and L. T. Jin, *Biosens. Bioelectron.*, 2006, **21**, 1996.
18 I. Pastoriza-Santos, J. Perez-Juste, G. Kickelbick and L. M. Liz-Marzan, *J. Nanosci. Nanotechol.*, 2006, **6**, 453.
19 D. I. Uhlenhaut, P. Smith and W. Caseri, *Adv. Mater.*, 2006, **18**, 1653.
20 K. S. Giesfeldt, R. M. Connatser, M. A. De Jesus, P. Dutta and M. J. Sepaniak, *J. Raman Spectrosc.*, 2005, **36**, 1134.
21 A. J. Wang, J. J. Xu, Q. Zhang and H. Y. Chen, *Talanta*, 2006, **69**, 210.
22 C. X. Luo, Q. Fu, H. Li, L. P. Xu, M. H. Sun, Q. Ouyang, Y. Chen and H. Ji, *Lab Chip*, 2005, **5**, 726.
23 B. Wang, K. Chen, S. Jiang, F. Reincke, W. J. Tong, D. Y. Wang and C. Y. Gao, *Biomacromolecules*, 2006, **7**, 1203.
24 N. Bao, Q. Zhang, J. J. Xu and H. Y. Chen, *J. Chromatogr., A*, 2005, **1089**, 270.
25 M. Darder, K. Takada, F. Pariente, E. Lorenzo and H. D. Abruña, *Anal. Chem.*, 1999, **71**, 5530.
26 Q. Zhang, J. J. Xu and H. Y. Chen, *J. Chromatogr., A*, 2006, **1135**, 122.
27 B. D. Freeman and I. Pinnau, *Trends Polym. Sci.*, 1997, **5**, 167.
28 T. C. Merkel, V. I. Bondar, K. Nagai, B. D. Freeman and I. Pinnau, *J. Polym. Sci., Part B: Polym. Phys.*, 2000, **38**, 415.
29 J. D. Plessis, W. J. Pugh, A. Judefeind and J. Hadgraft, *Eur. J. Pharm. Sci.*, 2002, **15**, 63.
30 T. R. E. Simpson, Z. Tabatabaian, C. Jeynes, B. Parbhoo and J. L. Keddie, *J. Polym. Sci., Part A: Polym. Chem.*, 2004, **42**, 1421.
31 F. Seker, P. R. L. Malenfant, M. Larsen, A. Alizadeh, K. Conway, A. M. Kulkarni, G. Goddard and R. Garaas, *Adv. Mater.*, 2005, **17**, 1941.
32 A. Toth, I. Bertoti, M. Blazio, G. Banhegyi, A. Bognar and P. Szaplonczay, *J. Appl. Polym. Sci.*, 1994, **52**, 1293.
33 J. B. Jia, B. Q. Wang, A. G. Wu, G. J. Cheng, Z. Li and S. J. Dong, *Anal. Chem.*, 2002, **74**, 2217.
34 L. Olofsson, T. Rindzevicius, I. Pfeiffer, M. Kall and F. Hook, *Langmuir*, 2003, **19**, 10414.
35 T. Powell and J. Yoon, *Biotechnol. Prog.*, 2006, **22**, 106.
36 V. Carralero, M. L. Mena, A. Gonzalez-Cortes, P. Yanez-Sedeno and J. M. Pingarron, *Biosens. Bioelectron.*, 2006, **22**, 730.
37 C. X. Guo, P. Boullanger, L. Jiang and T. Liu, *Biosens. Bioelectron.*, 2007, **22**, 1830.
38 S. H. Chen, R. Yuan, Y. Q. Chai, L. Y. Zhang, N. Wang and X. L. Li, *Biosens. Bioelectron.*, 2007, **22**, 1268.